Biochimica et Biophysica Acta 1784 (2008) 1997–2003

Contents lists available at ScienceDirect

Biochimica et Biophysica Acta

journal homepage: www.elsevier.com/locate/bbapap

Thermal unfolding studies of a phytocyanin

Rita Guzzi [a,*], Luigi Sportelli [a], Katsuko Sato [b], Salvatore Cannistraro [c], Christopher Dennison [b,*]

[a] Laboratorio di Biofisica Molecolare, Dipartimento di Fisica, Università della Calabria, CNISM, Ponte P. Bucci, Cubo 31C, 87036 Rende (CS), Italy
[b] Institute for Cell and Molecular Biosciences, Medical School, Newcastle University, Newcastle upon Tyne NE2 4HH, UK
[c] Biophysics and Nanoscience Centre, CNISM, Facoltà di Scienze, Università della Tuscia, Largo dell'Università, I-01100, Viterbo, Italy

ARTICLE INFO

Article history:
Received 21 May 2008
Received in revised form 3 July 2008
Accepted 3 July 2008
Available online 17 July 2008

Keywords:
Umecyanin
Thermal unfolding
Calorimetry
Fluorescence
Lumry–Eyring model

ABSTRACT

The thermal stability of umecyanin, a stellacyanin from horseradish roots, has been investigated by differential scanning calorimetry, optical absorption and fluorescence spectroscopy at neutral and alkaline pH. Above pH 9 the Cu(II) protein experiences a blue shift of the main visible absorption band at ~600 nm and changes colour from blue to violet. The thermal transition of the protein is irreversible and occurs between 61.4 and 68.8 °C at pH 7.5 and between 50.7 and 57.4 °C at pH 9.8. The calorimetric data indicates that at both pH values the thermally induced transition of the protein between the native and denaturated states can be described in terms of the classical Lumry–Eyring unfolding model Native↔Unfolded→Final. The analysis of the reversible step in the unfolding pathway demonstrates a significant reduction in conformational stability (ΔG) of the alkaline form of the protein. Such a reduction is consistent with an enhanced flexibility of UMC at high pH and has mainly entropic character.

1. Introduction

Umecyanin (UMC) from horseradish roots belongs to the phytocyanins, a family of cupredoxins [small copper-containing electron transfer (ET) proteins] which are found in plants and whose exact physiological function is not known [1,2]. UMC has a cupredoxin topology consisting of eight β-strands (and two α-helices) arranged into two β-sheets forming a Greek key β-barrel structure [3–5]. UMC and other structurally characterised phytocyanins [1,2,6], possess a number of unusual features compared to the typical cupredoxins. These include a disulfide bridge connecting Cys57 and Cys91, close to the active site, and a twist in one of the β-sheets that makes the β-barrel more opened. The copper ion is more solvent exposed and is only ~4 Å from the surface of the molecule, coordinated by the $N^{\delta 1}$ of His44 and His90, the S^{γ} from Cys85 and the $O^{\varepsilon 1}$ of Gln95 in a distorted tetrahedral arrangement in UMC. An axial Gln ligand is a feature unique to the stellacyanin sub-class of the phytocyanins [2,3,6]. Unlike other members of the cupredoxin family, both His ligands are solvent exposed in phytocyanins [3,5,6] which may favour interactions with small molecule redox partners [1,3,4]. UMC readily undergoes ET with redox protein partners [7]. Previous studies have shown that UMC, like other phytocyanins [8–10], undergoes an alkaline transition characterised by the protein changing from its characteristic blue colour [due to a S(Cys)→Cu(II) ligand to metal charge transfer (LMCT) transition at ~600 nm] at neutral pH to violet at pH>9 (the LMCT band shifts to ~580 nm at pH ~11). EPR [11], ^{1}H NMR [9,12] and resonance Raman [13] spectra are all influenced by this transition. Although the cause of this effect has not been identified, a number of possibilities have been suggested. In particular, a change in the coordination mode of the axial Gln ligand [14,15] and the deprotonation of a Lys residue close to the active site [16,17] were thought to be responsible for this effect. These possibilities have been disproved by site-directed mutagenesis studies [11] and deprotonation of a His ligand has been implicated [11,13,18]. Alteration of the secondary structure due to the supposed high flexibility of phytocyanins [8] has been suggested as being responsible for the alkaline transition.

Local conformational changes inducing an overall reorganization of the protein could in turn have an effect on thermostability. Information about the energetics of a protein can be obtained by means of thermal denaturation studies. Differential scanning calorimetry (DSC) is one of the most useful methods for assessing protein thermal behaviour and to obtain thermodynamic parameters of folding–unfolding transitions. A small monomeric protein should, ideally, unfold in a two-state reversible process. However, many proteins are unable to refold to the native state due to intermolecular aggregation and degradative covalent reactions occurring at temperatures higher than the melting temperature [19–21]. It is generally assumed that the slow kinetic nature of these irreversible processes, as observed by their dependence on the heating rate, allow separation of the reversible and irreversible steps [19,22].

In this study DSC, optical absorption and fluorescence spectroscopy have been used to investigate the thermally induced

* Corresponding authors. R. Guzzi is to be contacted at Laboratorio di Biofisica Molecolare, Dipartimento di Fisica, Università della Calabria, CNISM, Ponte P. Bucci, Cubo 31C, 87036 Rende (CS), Italy. Tel.: +39 0984 496077; fax: +39 0984 494401. C. Dennison, Institute for Cell and Molecular Biosciences, Medical School, Newcastle University, Newcastle upon Tyne NE2 4HH, UK. Tel.: +44 191 222 7127; fax: +44 191 222 7424.
E-mail addresses: guzzi@fis.unical.it (R. Guzzi), christopher.dennison@newcastle.ac.uk (C. Dennison).

1570-9639/$ – see front matter © 2008 Elsevier B.V. All rights reserved.
doi:10.1016/j.bbapap.2008.07.005

denaturation of UMC at neutral and alkaline pH. This is the first investigation of this kind on a phytocyanin. The results demonstrate that the thermal stability of the protein can be described by the two step Lumry–Eyring model including a reversibly unfolded intermediate state followed by an irreversible step. The disulfide bridge in phytocyanins contributes to the overall stability of their fold. At alkaline pH the protein's thermostability, considered in terms of denaturation temperature as well as Gibbs free energy change (ΔG), is lower than at neutral pH.

2. Materials and methods

2.1. Materials

UMC was expressed in *Escherichia coli* and purified as described previously [12]. For all experiments the protein was in 20 mM phosphate at pH 7.5. To raise the pH, small quantities of NaOH were added to UMC solutions. The pH value was measured with a Mettler Toledo pH meter. Protein concentrations were determined spectroscopically using an ε_{606} of 4300 M^{-1} cm^{-1} [12] and typically ranged between 20 and 30 μM.

2.2. Differential scanning calorimetry (DSC)

DSC experiments were performed on a VP-DSC MicroCalorimeter (MicroCal, Inc.) which has cell volumes of 0.52 mL and a temperature resolution of 0.1 °C. Oxidised protein samples were extensively degassed before measurements. To obtain a reproducible baseline, at least four scans with buffer in both the sample and reference cells were performed. The sample cell was loaded with protein and equilibrated for 30 min at 20 °C. Heating scans from 20 to 100 °C were obtained at scan rates of 15, 30, 60 and 90 °C h^{-1}. The temperature was then decreased to 20 °C before rescanning the sample. All data were analysed using the Origin software package (MicroCal). The reversibility of the transition was checked by performing a second scan with a previously heated sample. In addition, protein scans in which the temperature range of the first run was limited either to the maximum temperature of the Cp or to the end of the endothermic peak were also carried out.

2.3. Spectroscopy

Optical thermal profiles were acquired using a JASCO 7850 UV/Vis spectrophotometer equipped with a Peltier thermostated cell (model TPU-436, precision ±0.5 °C) and an EHC-441 temperature programmer. Quartz cuvettes with a 1 cm optical path length were used throughout. The absorbance at a fixed wavelength (usually the visible λ_{max} at ~600 nm) was followed over a temperature range from 20 to 80 °C at scan rates of 15, 30, 60 and 90 °C h^{-1}. At the end of each experiment, the temperature was lowered to 20 °C and a spectrum recorded to check for refolding. Fluorescence spectra were obtained with a Perkin-Elmer LS 50B spectrofluorimeter equipped with a PTP-1 Peltier Temperature Programmer using an excitation wavelength of 295 nm. The temperature was scanned from 20 to 80 °C at 60 °C h^{-1} and was measured directly with a YSI thermistor dipped into the cuvette. Emission spectra were recorded at 400 nm min^{-1}. Data were corrected for the sloping baselines from the folded and unfolded state of the protein and normalized to calculate the fraction of folded protein [23].

3. Results and discussion

3.1. Calorimetric investigations provide a quantitative analysis of the effect of the alkaline transition on the thermal stability of UMC

In Fig. 1A the DSC profile of Cu(II) UMC at pH 7.5 recorded at a scan rate of 60 °C h^{-1} is compared with the corresponding thermogram of

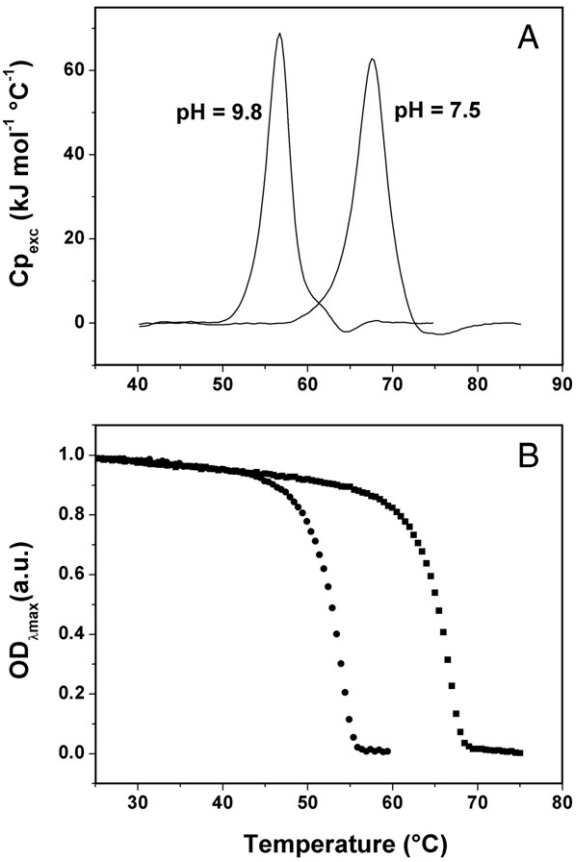

Fig. 1. (A) DSC thermograms and (B) normalized plots of absorbance at the wavelength of maximum intensity ($OD_{\lambda max}$) in the Vis region (606 nm at pH 7.5 and 594 nm at pH 9.8) against temperature for Cu(II) UMC in 20 mM phosphate at pH 7.5 (■) and 9.8 (●). In both cases the heating rate is 60 °C h^{-1}.

the protein at pH 9.8. In both cases the main features are an endothermic peak with T_{max} values of 67.5 and 56.7 °C respectively, and a smaller exothermic peak at higher temperatures. The exothermic peak is always observed in thermal unfolding studies of copper proteins [21,24,25] and has been attributed to aggregation processes occurring at $T > T_{max}$. Exothermic peaks have also been found for other proteins, such as insulin [20] and β-lactoglobulin [26] when studied under conditions favouring aggregation (high protein concentration). At alkaline pH the main endothermic peak is sharper than that obtained at neutral pH, indicating enhanced cooperativity of the thermal transition. Furthermore, a small shoulder is present on the high temperature side of the endothermic peak and a similar shoulder/peak has been found in the DSC thermograms of other cupredoxins including plastocyanin [21,27,28] and amicyanin [25] and is thought to be due to the formation of dimers during thermal melting. At alkaline pH the T_{max} of UMC is much lower than at neutral pH. Such destabilization may be related to a less stable conformation of UMC at high pH and also increased negative charge (an increased 5– charge is estimated between pH 7.5 and 9.5). A comparative analysis of the T_{max} at neutral pH with those obtained for other cupredoxins reveals that the value for UMC is equal to that of amicyanin [25], which has the same number of amino acids (106). However, because UMC and all other structurally characterised phytocyanins have a somewhat more open β-sandwich structure [3,5,29] compared to other cupredoxins, it is reasonable to assume that the presence of the disulfide bridge, which is an important distinctive structural element in UMC, could contribute to protein thermostability. A previous study [24] on the disulfide depleted azurin variant (Cys3Ala/Cys26Ala) has shown that the disulfide bond, which is located at the opposite end of the β-barrel to the copper site, significantly contributes to the high

stability of this cupredoxin (T_{max} for the SS depleted variant is 21 °C lower than for the wild type protein). We therefore assume that the phytocyanin fold is less stable than that of a 'standard' cupredoxin and that the disulfide close to the active site enhances stability.

The reversibility of the thermal transition was tested by performing a second scan on protein samples heated to the end of the endothermic peak or to the temperature of maximum heat capacity (T_{max}) [30]. The scan rate in all reversibility experiments was 90 °C h^{-1}. When the final temperature of the first scan is stopped immediately after the endothermic peak, no heat absorption was detected during the reheating run. When the first scan is interrupted at T_{max}, partial reversibility is found. The reversibility of the fraction of protein denaturated was calculated and expressed as a reversibility parameter which is defined as the ratio of calorimetric enthalpy (area under the curve) of the rescan with respect to that of the initial scan at the maximum temperature (T_H), [$\Delta H_c(T_H)$ 2nd scan/$\Delta H_c(T_H)$ 1st scan] [30,31]. In particular, at neutral pH when the first scan has been interrupted at T_H=68.8 °C a reversibility of 47% is obtained. Reversibility decreases as the maximum temperature of the initial scan increases. In fact, when the scan is stopped beyond the endothermic peak, at T_H=70.5 °C, only a small DSC signal is recorded in the second scan and reversibility drops to 7%. At high pH when the first scan was stopped at T_H=57.4 °C the second scan exhibits only 19% refolding. However, both the endothermic and exothermic peaks are still present in the rescan. One possible explanation of the lower degree of reversibility observed for the high pH form of UMC is that the final temperature of the first scan, T_H, is higher than the temperature needed for disruption of the copper site (T_t), which at the scan rate of 90 °C h^{-1} is 55.5 °C (*vide infra* and see Table 1). Thermal irreversibility in monomeric proteins is mainly ascribed to degradation reactions occurring at temperatures higher than T_{max} and to the presence of dissolved molecular oxygen in the solution [21,30,32,33]. The spontaneous reaction of free Cys residues with O_2 could promote the formation of oxidised sulphur species [32,34]. Moreover, the presence of a metal ion probably exacerbates the situation as it can promote protein aggregation. In fact, when the copper ion was removed in the cupredoxin pseudoazurin, the reversibility of protein unfolding is close to 100% and the transition could be described by a two-state model [35].

Irreversible processes associated with thermal denaturation of proteins are generally sensitive to the scan rate because they are under kinetic control. The scan rate dependence of the DSC profiles of UMC at pH 7.5 and 9.8 is shown in Fig. 2A and B, respectively. The data show that in both cases there is a progressive shift in the T_{max} to higher temperatures as the scan rate is increased. At the same time, the amplitude of the exothermic peak decreases with increasing scan rate and is almost absent at 90 °C h^{-1} at pH 9.8 (see Fig. 2B). In addition, the symmetry of the curves also increases as the scan rate is raised indicating a reduction in distortions of the thermal profile due to the irreversible processes. The reduction of the amplitude of the exothermic peak at higher scan rates indicates that this irreversible process is scan rate dependent and could, in principle, be eliminated by going to an infinite scan rate (not experimentally accessible). The thermodynamic analysis of the protein unfolding process requires that the thermal transition is reversible, which is partially verified for UMC as in the reversibility tests we have found some refolding (*vide supra*). Thermal denaturation of a protein is usually discussed in terms of the Lumry–Eyring model, $N \underset{k_{-1}}{\overset{k_1}{\rightleftarrows}} U \xrightarrow{k_2} F$, which includes two steps; (i) reversible unfolding of the native (N) protein to the unfolded (U) state and (ii) irreversible alteration of U to the final (F) form, that is unable to refold to N. When $k_2 \gg k_{-1}$, only the N and F states are significantly populated and the denaturation process can be considered using a one-step irreversible model following first order kinetics. This is not the case for UMC denaturation since there is some refolding which cannot occur if denaturation follows the simple one-step irreversible model. This means that the irreversible step is slower than reversible unfolding over the temperature range of the transition and therefore a thermodynamic analysis is appropriate [31,36]. Under this condition the experimental DSC profiles have been fitted using a non two-state model in which the heat capacity curve can be written as [19]:

$$Cp_{exc} = \frac{\Delta H \Delta H^{VH}}{RT^2} \frac{K}{(1-K)^2} \quad (1)$$

where the equilibrium constant $K = \exp\left[-\frac{\Delta H^{VH}}{R}\left(\frac{1}{T}-\frac{1}{T_{1/2}}\right)\right]$, ΔH^{VH} is the van't Hoff enthalpy, which may be different from the calorimetric enthalpy ΔH, and $T_{1/2}$ is the transition temperature when K=1. Since the high temperature side of the experimental DSC profiles is distorted by aggregation, and we are interested only in the reversible

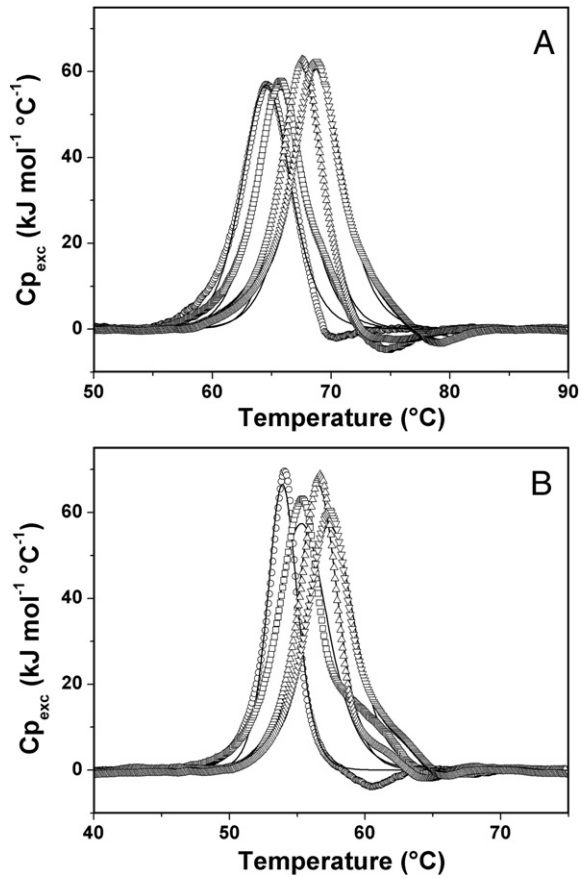

Fig. 2. Scan rate dependence of the DSC profiles of Cu(II) UMC at (A) pH 7.5 and (B) pH 9.8. The experimental curves are shown as symbols ((○) 15, (□) 30, (△) 60, (▽) 90 °C h^{-1}), whereas simulations derived using the non two-state model (Eq. (1), see text) are shown as solid lines. The simulation parameters are listed in Table 2.

Table 1
The influence of scan rate on the maximum heat of absorption temperature (T_{max}) and the Vis transition temperature (T_t) for Cu(II) UMC in 20 mM phosphate at pH 7.5 and 9.8

Scan rate (°C h^{-1})	DSC		Vis	
	T_{max} (°C)[a]		T_t (°C)[b]	
	pH 7.5	pH 9.8	pH 7.5	pH 9.8
15	64.6	54.1	62.4	50.7
30	65.7	55.4	63.5	51.7
60	67.5	56.7	67.0	53.9
90	68.8	57.4	68.0	55.5

[a] The estimated error on the T_{max} values is ±0.1 °C.
[b] The estimated error on the T_t values is ±0.5 °C.

part of the unfolding process, fits have been restricted to the main endothermic peak. The results are shown in Fig. 2 as solid lines and the fitting parameters are listed in Table 2. The ΔH values at alkaline pH are lower than those at neutral pH according to a weakened protein structure at high pH as also suggested by dynamic light scattering results which report an increase of the overall UMC size [13].

3.2. Thermal behaviour of UMC monitored by Vis absorption

The characteristic blue colour of the type 1 copper site of UMC is due to a S(Cys85)→Cu(II) LMCT transition, which gives rise to the optical absorption band at 606 nm at neutral pH. Upon increasing the pH to 9.8 the maximum absorption is blue shifted to 594 nm. Conformational changes within the copper site environment that alter the Cu(II)–S(Cys) interaction can be monitored using visible absorbance. The variation of the normalized intensity of this LMCT band of Cu(II) UMC at pH 7.5 as a function of the temperature (scan rate 60 °C h^{-1}) is shown in Fig. 1B. The sigmoidal shape of this thermal profile is typical of a two-state transition. The intensity of the optical absorption is only slight reduced (by about 10%) from the starting temperature during the pre-transition region, which is followed by an abrupt decrease to zero. The transition region is very narrow with a temperature range of approximately 10 °C. Increasing the scan rate from 15 to 90 °C h^{-1} has no effect on the shape of the thermal profiles, but does influence the transition temperature, T_t, which varies from 62.4 to 68.0 °C, respectively at pH 7.5 (Fig. 3A and Table 1). The increase of T_t with scan rate is further indication of a kinetically controlled thermal transition as observed in the DSC experiments. The denaturation process of UMC is accompanied by bleaching of the protein solution and the blue colour is not recovered by cooling the sample to room temperature. This effect can be ascribed to changes in the tertiary structure of the protein, which permanently alters the copper coordination environment.

When the pH of UMC is increased to 9.8 the temperature dependence of the absorbance at the visible λ_{max} indicates a significant decrease in protein stability (Fig. 1B). In fact, T_t determined at alkaline pH is about 12 °C lower than that at neutral pH. Such a reduction is maintained at all scan rates (Fig. 3B and Table 1), but does not affect the shapes of the thermal profiles. The reduced thermal stability indicates that the Cu–S(Cys) interaction is more easily disrupted at alkaline pH. This result is consistent with a series of previous experimental findings. In particular, dynamic light scattering experiments have shown that as the pH is raised, the hydrodynamic diameter of UMC increases by ~50% [13]. This change is reversible when neutral pH is restored. Moreover, resonance Raman and NMR investigation of the alkaline transition of UMC have provided interesting information about modifications within the copper environment as a consequence of the alkaline transition. In fact, the Cu(II)–S(Cys) bond length increases whereas Cu(II)–N(His) bonding strengthens at high pH [9,13].

3.3. Determination of activation parameters

Kinetic stability is an important aspect of irreversible protein denaturation [30]. Information on kinetics of the denaturation pathway can be obtained from the scan rate dependent thermal profiles recorded in DSC and Vis experiments. Using the scan rate dependence of T_{max} it is possible to derive the apparent activation energy (E_a) according to the following equation:

$$\ln\left(v/T_{max}^2\right) = C - E_a/RT_{max} \quad (2)$$

where v is the scan rate. From the slope of the linear plot of $\ln(v/T^2_{max})$ against $1/T_{max}$ we obtain E_a values of 361 ± 18 and 434 ± 27 kJ mol^{-1} for UMC at pH 7.5 and 9.8, respectively. The higher E_a at alkaline pH is in agreement with the sharper DSC profiles under these conditions as E_a is inversely proportional to peak width [31]. When T_{max} is substituted by T_t in Eq. (2), we can calculate the apparent E_a related to disruption of the active site. In this case E_a values of 243 ± 27 and 285 ± 25 kJ mol^{-1}, respectively are obtained for the neutral and alkaline forms of UMC. The E_a determined for the copper site environment is also higher for the alkaline form, suggesting an increase in the kinetic stability with increasing pH.

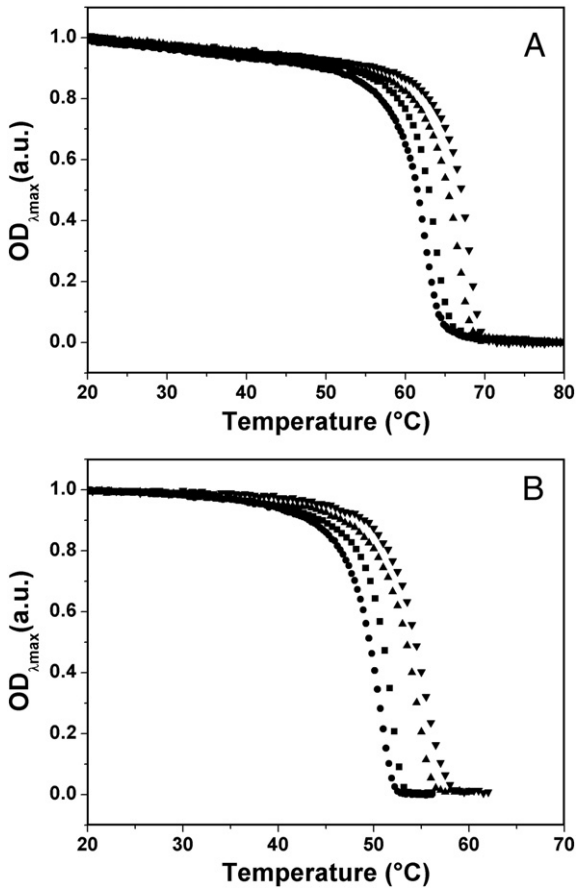

Fig. 3. Dependence on scan rate of normalized $OD_{\lambda max}$ profiles for Cu(II) UMC at (A) pH 7.5 and (B) pH 9.8 at scan rates of 15 (●), 30 (■), 60 (▲) and 90 (▼) °C h^{-1}.

Table 2
Scan rate dependence of the $T_{1/2}$ and ΔH values obtained from the non two-state model fit of DSC profiles for Cu(II) UMC in 20 mM phosphate at pH 7.5 and 9.8

Scan rate (°C h^{-1})	$T_{1/2}$ (°C)		ΔH (kJ mol^{-1})	
	pH 7.5	pH 9.8	pH 7.5	pH 9.8
15	64.54 ± 0.02	53.91 ± 0.01	312.2 ± 1.7	197.3 ± 1.7
30	65.75 ± 0.02	55.32 ± 0.03	320.2 ± 2.5	298.4 ± 3.7
60	67.45 ± 0.02	56.54 ± 0.02	299.3 ± 2.9	259.6 ± 2.2
90	68.74 ± 0.03	57.39 ± 0.03	360.0 ± 3.3	280.5 ± 2.1

3.4. Thermal behaviour of UMC monitored by fluorescence

Intrinsic fluorescence from a Trp residue is highly sensitive to the micro-environment of this residue and is widely used to investigate changes in protein tertiary structure [37]. A more polar surrounding generally results in the Trp emission shifting to longer wavelength (red shifted), whilst a more hydrophobic environment results in a blue shift. Fig. 4 shows the fluorescence spectra of Cu(II) UMC at pH 7.5 (solid thick line) and 9.8 (solid thin line), using an excitation wavelength of 295 nm. Both of these spectra were recorded at room temperature, i.e. with the protein in the native state, and exhibit a

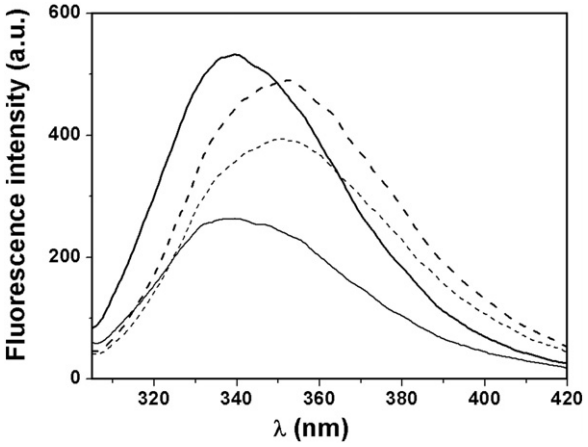

Fig. 4. Fluorescence spectra of Cu(II) UMC at pH 7.5 (thick line) and 9.8 (thin line). Spectra shown as solid lines were recorded at 25 °C whilst those shown as dashed lines were obtained at 63 and 70 °C at neutral and alkaline pH, respectively i.e. after the thermal transition.

large emission peak centered at ~340 nm which indicates that both Trp11 and Trp23 in UMC are solvent exposed. The absence of any influence of pH on the fluorescence signal suggests that the alkaline transition does not change the micro-environments of both Trp residues. Upon increasing temperature, the position of the maximum emission is progressively shifted up to ~350 nm (dashed lines), consistent with protein unfolding [37]. Fig. 5A shows the variation in the fluorescence intensity at the emission maximum (340 nm) as a function of temperature at the two pH values studied. The overall trends of the two profiles are similar, although some differences do exist. In particular, at neutral pH the intensity of emission is lowered upon increasing temperature, whereas at alkaline pH the fluorescence increases at elevated temperatures. This result suggests that the final state could be different at the two pH values. In particular, in agreement with the DSC results UMC shows a higher tendency to aggregate as the temperature is increase at alkaline pH.

The typical unfolding curves shown in Fig. 5A were normalized and corrected for the slopes of the baselines for the folded and unfolded states to calculate the fraction of folded protein (Fig. 5B). The normalized profiles were fitted with a Boltzmann sigmoidal function;

$$I(T) = \frac{I_1 - I_2}{1 + e^{(T-T_f)/d}} + I_2 \quad (3)$$

where I_1 and I_2 are the limiting intensity values in the native and unfolded states, respectively, T_f is the transition temperature between the two conformational states corresponding to $I(T_f) = \frac{I_1 + I_2}{2}$ and d is an exponential decay constant. The parameters for the fit shown in Fig. 5B give a T_f value of 60.8±0.1 °C and a d of 1.67±0.04 °C^{-1} for UMC at pH 7.5. The corresponding values for UMC at alkaline pH are 54.9±0.1 °C and 1.20±0.04 °C^{-1}. The transition region at alkaline pH is steeper, characterised by a smaller value of d, suggesting a more cooperative thermal transition which occurs at lower temperature which is in agreement with the DSC studies. At both pH values, returning the protein samples to room temperature after the thermal scan results in the fluorescence intensity significantly increasing to three times its starting value. The maximum emission shifts to 345 nm, a value intermediate between the initial value and that at high temperature. This blue shift of the λ_{max} of emission and the intensity increases both indicate a final state of the protein where the Trp residues are more shielded from the solvent with respect to the state at high temperature, but more exposed than in the folded protein, probably due to aggregation of the denaturated protein.

Comparing the transition temperatures determined by fluorescence and optical absorption at a scan rate of 60 °C h^{-1} highlights that T_f is about 6 °C lower than T_t at neutral pH. Because solvent accessibility is the major factor determining the fluorescence of the Trp residues, the data suggest that the fluorescence change may reach its limiting value before the copper center is disrupted. The transition temperatures are very similar, within experimental error, when measured by the different techniques at alkaline pH. This is compatible with a general weakening of the interactions in the

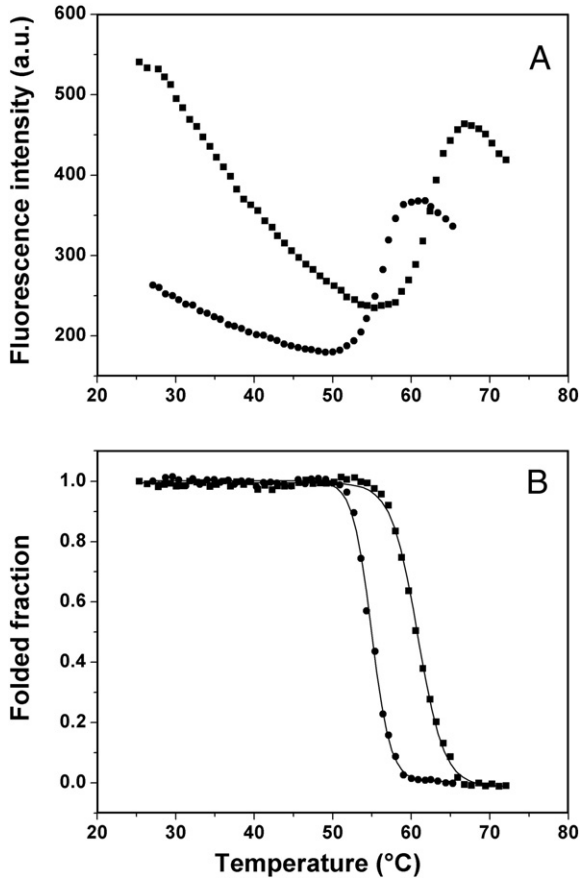

Fig. 5. (A) Thermal unfolding of Cu(II) UMC at pH 7.5 (■) and 9.8 (●) followed using the fluorescence intensity at the wavelength of maximum emission (340 nm). The scan rate in both cases was 60 °C h^{-1}. (B) Normalized fluorescence thermal unfolding curves (see Materials and methods) where the solid line represents the fit of the experimental data to Eq. (3).

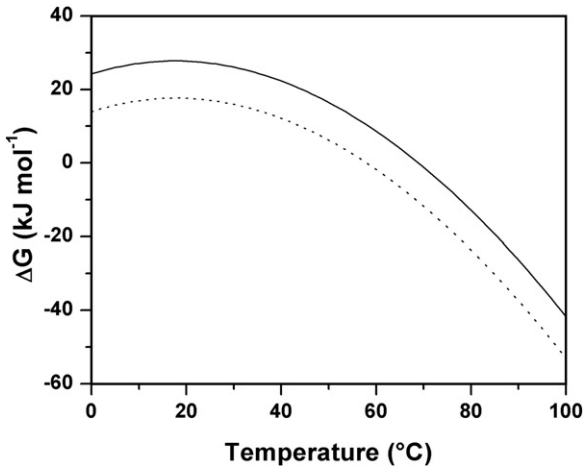

Fig. 6. Temperature dependence of the Gibbs free energy of unfolding (ΔG) for Cu(II) UMC at neutral (solid line) and alkaline (dashed line) pH.

Table 3
Thermodynamic parameters for Cu(II) UMC at pH 7.5 and 9.8 at 20 °C

pH	ΔH kJ mol^{-1}	ΔS kJ mol^{-1} K^{-1}	$T\Delta S$ kJ mol^{-1}	ΔG kJ mol^{-1}
7.5	44.5	0.057	16.7	27.7
9.8	38.7	0.072	21.1	17.5

whole protein structure as the pH is increased, indicating that the two regions, the copper site and the Trp environment, directly explored by the two techniques have the same thermostability.

3.5. Thermodynamic analysis of the unfolding process

The conformational stability of a protein is described by the temperature dependence of the Gibbs free energy [38,39]:

$$\Delta G(T) = \Delta H_U \frac{T_{1/2}-T}{T_{1/2}} - \Delta Cp\left(T_{1/2}-T\right) + T\Delta Cp \ln\frac{T_{1/2}}{T} \quad (4)$$

The irreversibility of the DSC transition prevents the experimental determination of ΔCp, i.e. $Cp_U - Cp_N$, since Cp at the offset temperature is related to the final (F) and not the unfolded (U) state. In this case ΔCp can be calculated by means of theoretical methods based on the amino acid sequence of the protein [40,41]. The value obtained for UMC, using the Murphy and Gill model, is 6.5 kJ mol^{-1} K^{-1} which along with the ΔH and $T_{1/2}$ values obtained from the simulation of the DSC profiles at the highest scan rate have been used in Eq. (4) to calculate the temperature dependencies of ΔG at pH 7.5 and 9.5 shown in Fig. 6. The two functions follow a similar trend with lower values for the curve for UMC at alkaline pH. The ΔG values at 20 °C are 27.7 and 17.5 kJ mol^{-1} at pH 7.5 and 9.8 respectively, indicating that the alkaline transition is characterised by a dramatic decrease in the conformational stability of UMC. If we consider the enthalpic contribution to ΔG, at 20 °C there is a variation of ~6 kJ mol^{-1} (Table 3). The similarity of the unfolding enthalpy of UMC at the two pH values suggests that the reduced stability of the protein at high pH arises mainly from entropic effects. In fact, the ΔS values at 20 °C is higher for UMC at pH 9.8 (Table 3) and the entropic gain is 0.015 kJ mol^{-1} K^{-1}. The two terms which contribute to the unfolding entropy are the conformational (ΔS_{conf}) and solvent (ΔS_{solv}) entropies that are positive and negative respectively. To explain the entropy gain at alkaline pH it can be hypothesized that a reduction of solvation contributes to the unfolding entropy. In fact, the solvation entropy depends on solvent accessible surface area differences (ΔASA), between the native and denatured states [39]. The observed increase in the hydrodynamic radius of UMC at alkaline pH [13] indicates an increase in the ASA of the native state, and therefore ΔASA is lower at pH 9.8 than at neutral pH.

4. Conclusions

The combination of a range of experimental techniques which monitor different regions of the protein has allowed investigation of the thermal behaviour of UMC at ~neutral and alkaline pH values. The denaturation pathway can be described in terms of a two step N↔U→F unfolding model analogous to that already used for other cupredoxins. Changes in pH do not affect the unfolding pathway but strongly influence the conformational stability which decreases dramatically at alkaline pH. The reduced stability at high pH is related to an enhanced protein flexibility and has been mainly explained in terms of an entropy gain. From the transition temperatures obtained by DSC, Vis and fluorescence experiments, it appears that UMC denaturation starts with the destabilization of the Trp residues environments, followed by the disruption of the copper site and simultaneous unfolding of the whole protein. At alkaline pH the changes at the copper site occur almost simultaneously with the Trp environment changes with both preceding global protein unfolding.

Acknowledgements

This work has been partly supported by PRIN-MUR project (n.2006028219); BBSRC (Grant 13/B16498), Newcastle University; MiUR ex 60%, University of Calabria.

References

[1] A.M. Nersissian, S.L. Shipp, Blue copper-binding domain, Adv. Prot. Chem. 60 (2002) 271–340.
[2] C. Dennison, Investigating the structure and function of cupredoxins, Coord. Chem. Rev. 24 (2005) 3025–3054.
[3] P.J. Hart, A.M. Nersissian, R.G. Herrmann, R.M. Nalbandya, J.S. Valentine, D.A. Eisenberg, Missing link in cupredoxins: crystal structure of cucumber stellacyanin at 1.6 angstrom resolution, Protein Sci. 5 (1996) 2175–2181.
[4] J.M. Guss, E.A. Merritt, R.P. Phizackerely, H.C. Freeman, The structure of a phytocyanin, the basic blue copper from cucumber refined at 1.8 angstrom resolution, J. Mol. Biol. 262 (1996) 686–705.
[5] M. Koch, M. Velarde, M.D. Harrison, S. Echt, M. Fisher, A. Messerschmidt, C. Dennison, Crystal structures of oxidized and reduced stellacyanin from horseradish root, J. Am. Chem. Soc. 127 (2005) 158–166.
[6] A.M. Nersissian, C. Immoos, M.G. Hill, P.J. Hart, G. Williams, R.G. Herrmann, J.S. Valentine, Uclacyanins, stellacyanins, and plantacyanins are distinct subfamilies of phytocyanins: plant-specific mononuclear blue copper proteins, Protein Sci. 7 (1998) 915–1929.
[7] K. Sato, P.B. Crowley, C. Dennison, Transient protein interactions between cytochrome *f* and the phytocyanin umecyanin, ChemBioChem. 8 (2007) 732–735.
[8] C.O. Fernandez, A.I. Sannazzaro, A.J. Vila, Alkaline transition of *Rhus vernicifera* stellacyanin, un unusual blue copper protein, Biochemistry 36 (1997) 10566–10570.
[9] C. Dennison, A.T. Lawler, Investigation of the alkaline and acid transition of umecyanin, a stellacyanin from horseradish roots, Biochemistry 40 (2001) 3158–3166.
[10] C. Dennison, M.D. Harrison, A.T. Lawler, Alkaline transition of phytocyanins: a comparison of stellacyanin and umecyanin, Biochem. J. 371 (2003) 377–383.
[11] M.D. Harrison, S. Yanagisawa, C. Dennison, Investigating the cause of the alkaline transition of phytocyanins, Biochemistry 44 (2005) 3056–3064.
[12] C. Dennison, M.D. Harrison, The active-site structure of umecyanin, the stellacyanin from horseradish roots, J. Am. Chem. Soc. 126 (2004) 2481–2489.
[13] I. Delfino, K. Sato, M.D. Harrison, L. Andolfi, A.R. Bizzarri, C. Dennison, S. Cannistraro, Optical investigation of the alkaline transition in umecyanin from horseradish root, Biochemistry 44 (2005) 16090–16097.
[14] H. Thomann, M. Bernardo, M.J. Baldwin, M.D. Lowery, E.I. Solomon, Pulsed ENDOR study of the native and high perturbed forms of the blue copper site in stellacyanin, J. Am. Chem. Soc. 113 (1991) 5911–5913.
[15] B.A. Fields, J.M. Guss, H.C. Freeman, Three-dimensional model for stellacyanin, a "blue" copper-protein, J. Mol. Biol. 222 (1991) 1053–1065.
[16] M. van de Kamp, G.W. Canters, C.R. Andrew, J. Sanders-Loehr, C.J. Bender, J. Peisach, Effect of lysine ionization on the structure and electrochemical behaviour of the Met44→Lys mutant of the blue-copper protein azurin from *Pseudomonas aeruginosa*, Eur. J. Biochem. 218 (1993) 229–238.
[17] C. Dennison, G. Van Driessche, J. Van Beeumen, W. McFarlane, A.G. Sykes, Electron-transfer properties and active-site structure of the type 1 (blue) copper protein umecyanin, Chem. Eur. J. 1 (1996) 104–109.
[18] G. Battistuzzi, M. Bellei, C. Dennison, G. Di Rocco, K. Sato, M. Sola, S. Yanagisawa, Thermodynamics of the alkaline transition in phytocyanins, J. Biol. Inorg. Chem. 12 (2007) 895–900.
[19] M. Thorolfsson, B. Ibarra-Molero, P. Fojan, S.B. Petersen, J.M. Sanchez-Ruiz, A. Martinez, L-Phenylalanine binding and domain organization in human phenylalanine hydroxylase: a differential scanning calorimetry study, Biochemistry 41 (2002) 7573–7585.
[20] W. Dzwolak, R. Ravindra, R. Winter, Aggregation of bovine insulin probed by DSC/PPC calorimetry and FTIR spectroscopy, Biochemistry 42 (2003) 11347–11355.
[21] A. Sandberg, D.J. Harrison, B.G. Karlsson, Thermal denaturation of spinach plastocyanin: effect of copper oxidation state and molecular oxygen, Biochemistry 42 (2003) 10301–10310.
[22] I. Quesada-Soriano, F. Garcia-Maroto, L. Garcia-Fuentes, Kinetic study on the irreversible thermal denaturation of *Schistisoma japonicum* glutathione *s*-transferase, Biochim. Biophys. Acta 1764 (2006) 979–984.
[23] M.J. Feio, A. Diaz-Quintana, J.A. Navarro, M.A. De la Rosa, Thermal unfolding of plastocyanin from the mesophilic cyanobacterium *Synechocystis* sp. PCC 6803 and comparison with its thermophilic counterpart from *Phormidium laminosum*, Biochemistry 45 (2006) 4900–4906.
[24] R. Guzzi, L. Sportelli, C. La Rosa, D. Milardi, D. Grasso, M. Ph. Verbeet, G.W. Canters, A spectroscopic and calorimetric investigation on the thermal stability of the Cys3Ala/Cys26Ala azurin mutant, Biophys. J. 77 (1999) 1052–1063.
[25] J.K. Ma, G.R. Bishop, V.L. Davidson, The ligand geometry of copper determines the stability of amicyanin, Arch. Biophys. Biochem. 444 (2005) 27–33.
[26] S.M. Fitzsimons, D.M. Mulvihill, E.R. Morris, Denaturation and aggregation process in thermal gelation of whey proteins resolved by differential scanning calorimetry, Food Hydrocoll. 21 (2007) 638–644.

[27] R. Guzzi, L. Andolfi, S. Cannistraro, M. Ph. Verbeet, G.W. Canters, L. Sportelli, Thermal stability of wild type and disulfide bridge containing mutant of poplar plastocyanin, Biophys. Chem. 112 (2004) 35–43.
[28] A. Shosheva, A. Donchev, M. Dimitrov, G. Kostov, G. Toromanov, V. Getov, E. Alexov, Comparative study of the stability of poplar plastocyanin isoforms, Biochem. Biophys. Acta 1748 (2005) 116–127.
[29] O. Einsle, Z. Mehrabian, R. Nalbandyan, A. Messerschmidt, Crystal structure of plantacyanin, a basic blue cupredoxin from spinach, J. Biol. Inorg. Chem. 5 (2000) 666–672.
[30] D. Rodriguez-Larrea, B. Ibarra-Molero, L. de Maria, T.V. Borchert, J.M. Sanchez-Ruiz, Beyond Lumry–Eyring: an unexpected pattern of operational reversibility/irreversibility in protein denaturation, Proteins 70 (2008) 19–24.
[31] J.R. Lepock, H.E. Frey, R.A. Hallewell, Contribution of conformational stability and reversibility of unfolding to the increased thermostability of human and bovine superoxide dismutase mutated at free cysteines, J. Biol. Chem. 265 (1990) 21612–21618.
[32] A. Sandberg, J. Leckner, Y. Shi, F.P. Schwarz, B.G. Karlsson, Effects of metal ligation and oxygen on the reversibility of the thermal denaturation of *Pseudomonas aeruginosa* azurin, Biochemistry 41 (2002) 1060–1069.
[33] A. Tigerstrom, F.P. Schwarz, B.G. Karlsson, M. Okvist, C. Alvarez-Rua, D. Maeder, F.T. Robb, L. Sjolin, Effects of a novel disulfide bond and engineered electrostatic interactions on the thermostability of azurin, Biochemistry 43 (2004) 12563–12574.
[34] C. Jacob, A.L. Holme, F.H. Fry, The sulfinic acid switch in proteins, Org. Biomol. Chem. 2 (2004) 1953–1956.
[35] A. Stirpe, L. Sportelli, R. Guzzi, A comparative investigation of the thermal unfolding of pseudoazurin in the Cu(II)-holo and apo form, Biopolymers 83 (2006) 487–497.
[36] M. Espina, S.F. Ausar, R. Middaugh, W.D. Picking, W.L. Picking, Spectroscopic and calorimetric analyses of invasion plasmid antigen D (IpaD) from *Shigella flexneri* reveal the presence of two structural domains, Biochemistry 45 (2006) 9219–9227.
[37] M.R. Eftink, The use of fluorescence methods to monitor unfolding transitions in proteins, Biochemistry (Moscow) 63 (1998) 276–284.
[38] P.L. Privalov, Physical basis of the stability of the folded conformations of proteins, in: T.E. Creighton (Ed.), Protein Folding, W. H. Freeman and Co, New York, 1992, pp. 83–126.
[39] E. Freire, The thermodynamic linkage between protein structure, stability and function, Methods in Mol. Biol. 168 (2001) 37–68.
[40] P.K. Murphy, S.J. Gill, Solid model compounds and the thermodynamics of protein folding, J. Mol. Biol. 22 (1991) 699–709.
[41] D. Milardi, C. La Rosa, S. Fasone, D. Grasso, An alternative approach in the structure-based prediction of the thermodynamics of protein unfolding, Biophys. Chem. 69 (1997) 43–51.